JOURNAL OF GEOPHYSICAL RESEARCH, VOL. 113, C11011, doi:10.1029/2008JC004781, 2008

Explaining the patterns formed by ice floe interactions

Dominic Vella[1] and J. S. Wettlaufer[2]

Received 19 February 2008; revised 26 June 2008; accepted 18 July 2008; published 11 November 2008.

[1] We provide a quantitative explanation of the patterns commonly observed during the collision of two floating ice sheets (ice floes): simple rafting, finger rafting, or the formation of a pressure ridge. In particular, we analyze the equilibrium configurations of the ice in each of the two types of rafting and show that these are only possible if the ice thickness is below a threshold value that we determine in terms of the strength and elastic modulus of the ice. We construct a regime diagram to characterize the regions of thickness-strength parameter space for which each type of deformation can occur. Using typical values for the strength of sea ice, we find that finger rafting can only occur in ice with thickness $\lesssim$8 cm, and simple rafting can typically only occur in ice with thickness $\lesssim$21 cm. These estimates are quantitatively consistent with most field observations reported in the literature. Finally, by quantifying two common complications that occur in reality, we are also able to account for some of the discrepancies between theory and observation that remain. We show that the presence of rubble may allow ice with a thickness of up to 1 m to perform simple rafting, but multiple rafting of thin sheets does not increase the maximum rafting thickness.

Citation: Vella, D., and J. S. Wettlaufer (2008), Explaining the patterns formed by ice floe interactions, *J. Geophys. Res.*, *113*, C11011, doi:10.1029/2008JC004781.

1. Introduction

[2] Floating ice in polar seas and northern lakes is perpetually subject to wind and water stresses that drive their deformation. These forces, and their mediation by the ice itself, are responsible for creating the mosaic of individual ice sheets, or ''floes'' that characterize sea ice as it evolves dynamically and thermodynamically. On the large scale these deformation processes, and the redistribution of ice thickness as it deforms, create the observed ice thickness distribution, which is described by an evolution equation that has been with us for more than 30 years [*Thorndike et al.*, 1975; *Wensnahan et al.*, 2007]. On the floe scale, the mechanical processes that underlie the transformation of ice from one thickness to that of another are described by three basic patterns of rafting and ridging. In this article, we study the conditions under which these different patterns occur.

[3] Ridging and rafting play a controlling role in the mechanical redistribution of sea ice thickness [*Thorndike et al.*, 1975; *Babko et al.*, 2002], and for thin ice they (along with other processes) alter the albedo of the ice cover significantly. For example, in rafting the ice doubles in thickness and so appears much whiter than surrounding ice. The floe-scale processes responsible for these patterns can therefore be viewed as the foundation for the constitutive behavior of the geophysical mosaic and have motivated a long-term effort to marry the scales of relevance. *Rothrock* [1975, p. 325] provided a succinct description of the matter:

[4] ''If we knew what the constitutive equation for pack ice should be, we would not need to pay attention to the mechanisms of floe interaction. But the simple fact is that we are not at all sure about the constitutive equation... we have turned to the study of these mechanisms —rafting, ridging, shearing, and opening— to deduce what we can about the large-scale mechanical behavior of pack ice.''

[5] Because the floe-scale regimes of deformation patterns are intrinsically interesting, and involve phenomena that extend to systems across a wide range of natural and technological systems, the potential implications of our simple theoretical treatment of colliding ice sheets extend beyond sea ice geophysics. While in this field we are motivated to help establish the foundations of the large-scale behavior of pack ice, it is hoped that the edifice is of some use in other fields.

[6] During simple rafting, one ice floe rides over the adjoining floe without the creation of a large amount of rubble. In finger rafting, rather than one floe riding over another, the two floes alternately ride over and under one another forming a series of interlocking fingers. Generically, these fingers have very sharp linear features that are particularly striking, as is the well-defined spacing of the fingers. Simple rafting and finger rafting are illustrated in Figures 1 and 2. Finally, the most destructive of the three families of patterns is the pressure ridge wherein the two ice floes break up as they collide thereby forming a ''sail'' and a ''keel'' of highly fractured ice blocks.

[7] In this article, we characterize quantitatively the conditions under which each of the three deformation patterns is observed. First, we discuss the transition between

[1]Institute of Theoretical Geophysics, Department of Applied Mathematics and Theoretical Physics, University of Cambridge, Cambridge, UK.
[2]Department of Geology and Geophysics and Department of Physics, Yale University, New Haven, Connecticut, USA.

0148-0227/08/2008JC004781$09.00

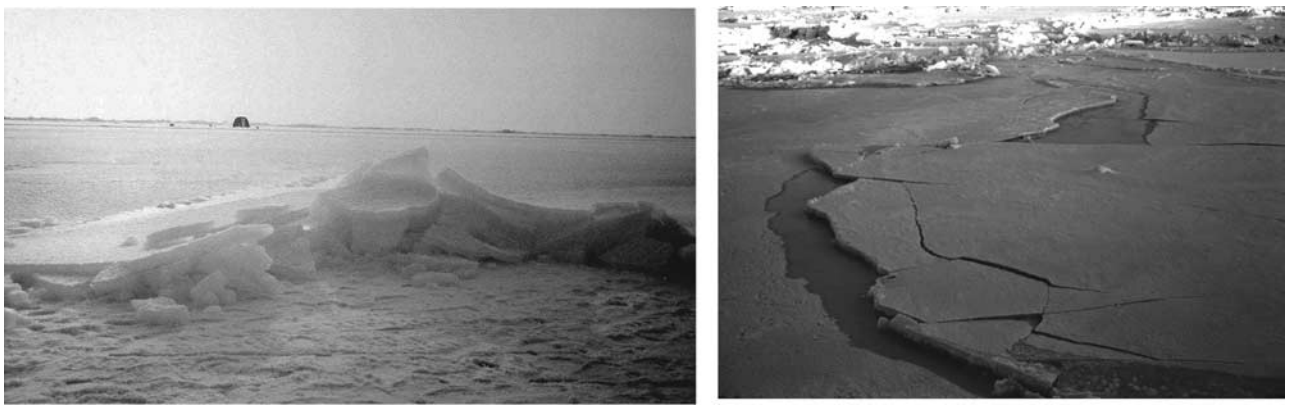

Figure 1. Photograph showing, left-hand side, an end-on view of simple rafting. The overriding floe has failed in places, suggesting a close link between simple rafting and pressure ridging. On the right-hand side we see a similar process from a different perspective (photograph courtesy of W. F. Weeks, *On Sea Ice*, submitted to University of Alaska Fairbanks Press, 2008).

simple rafting and pressure ridging, which was studied by *Matsuoka* [1972] and *Parmerter* [1975]. We present a simplified version of their model, which produces a very similar result. This simplified approach allows us to then consider more complicated situations, such as the effect of rubble covering the floe. Including the effect of this preloading at least partially explains the discrepancy reported between *Matsuoka*'s [1972] result and field observations [*Babko et al.*, 2002]. We also consider multiple rafting events and show that, surprisingly, these do not quantitatively alter the transition between rafting and ridging. Finally, we consider a very simplified model of finger rafting, which explains why this formation is only observed in very thin ice.

2. Simple Rafting Versus Pressure Ridging

[8] The photograph in Figure 1 suggests that simple rafting and pressure ridging are very closely related. Indeed, *Weeks and Kovacs* [1970] reported, on the basis of their field observations, that there appears to be a transition between simple rafting and ridging at a critical ice thickness. *Matsuoka* [1972] presented a model of simple rafting, which was developed further in the numerical study of *Parmerter* [1975]. These studies showed that there is a maximum ice thickness, h_c, above which ice cannot raft and must instead form a pressure ridge. Furthermore, they showed how h_c depends on the material properties of ice (specifically the Poisson ratio ν, Young's modulus E, and tensile strength, σ_m), the density of the underlying water, ρ_l, and the gravitational acceleration, g. In particular, they found that

$$h_c \approx 14.2 \frac{1-\nu^2}{\rho_l g} \frac{\sigma_m^2}{E}. \tag{1}$$

[9] In this section we present a simpler, analytic model of simple rafting to highlight the important physical principles that determine when simple rafting can occur. We note that the energetics and evolution of ridging have been studied by *Parmerter and Coon* [1972], *Rothrock* [1975], and *Hopkins* [1998]. Our work abuts theirs by providing conditions delineating between rafting and ridging.

2.1. An Analytical Model

[10] Consider two ice floes (with identical, constant thickness, h) in the configuration shown schematically in Figure 3: the two floes are on the brink of rafting. In this situation, a small portion of the lower floe may be submerged, as modeled by *Matsuoka* [1972], but here we shall neglect this possibility for simplicity. We also neglect any tension within the floes because, in equilibrium, this tension must be balanced by friction between the floes in the very small overlapping region, and hence must be small.

[11] With these simplifying assumptions, the height, $w(x)$, of the centerline of each floe above the water surface with respect to the horizontal coordinate x, is governed by the plate equation [*Mansfield*, 1989]

$$B\frac{\mathrm{d}^4 w}{\mathrm{d}x^4} = -\rho_s g h + \rho_l g\left(\frac{h}{2} - w\right) \tag{2}$$

Figure 2. Finger rafting in the Amundsen Sea. Photograph courtesy of Weeks (submitted manuscript, 2008).

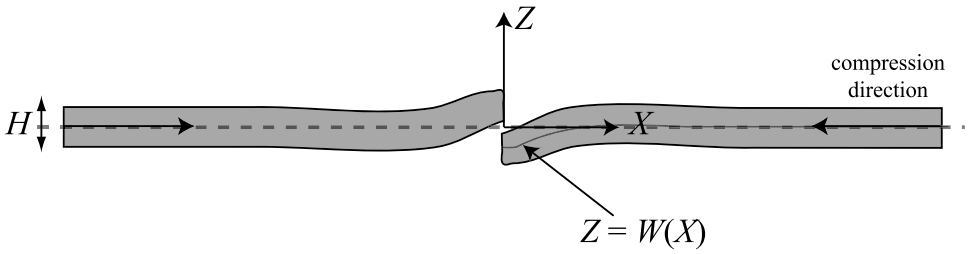

Figure 3. Schematic of two ice floes on the brink of rafting.

where

$$B \equiv \frac{Eh^3}{12(1-\nu^2)} \tag{3}$$

is the bending stiffness of the floe and ρ_s is the density of the solid (in this case ice). The first term on the right-hand side of equation (2) represents the weight per unit area of the ice floe, while the second term represents the upthrust due to the hydrostatic pressure in the liquid.

[12] In the following it will be convenient to work in nondimensional terms and so we nondimensionalize lengths using

$$\ell \equiv (B/\rho_l g)^{1/4}, \tag{4}$$

which is the length scale over which the deflection of the floe decays.

[13] With no forces other than gravity acting, the sheet will remain flat and float with $w = w_\infty \equiv h(1/2\text{-}\rho_s/\rho_l)$. For simplicity, therefore, we shall measure all vertical displacements relative to this equilibrium level and introduce the dimensionless variables

$$W \equiv (w - w_\infty)/\ell, \quad X \equiv x/\ell, \quad \text{and} \quad H \equiv h/\ell. \tag{5}$$

The shape of each floe is then governed by

$$\frac{\mathrm{d}^4 W}{\mathrm{d}X^4} + W = 0. \tag{6}$$

Solving equation (6) subject to the jump in plate height at $X = 0$:

$$W(0^-) - W(0^+) = H, \tag{7}$$

and the continuity of the first three derivatives of W at $X = 0$, we find that

$$W(X) = \begin{cases} \frac{H}{2} e^{X/\sqrt{2}} \cos\left(X/\sqrt{2}\right), & X < 0 \\ -\frac{H}{2} e^{-X/\sqrt{2}} \cos\left(X/\sqrt{2}\right), & X > 0. \end{cases} \tag{8}$$

[14] Since we are interested in when simple rafting fails, it is natural to examine the stress within the floe. From the theory of elasticity, the tensile stress within the floe is a function of the height z above the centerline. In dimensional terms, we have [*Mansfield*, 1989]

$$\sigma = -\frac{Ez}{1-\nu^2} \frac{\mathrm{d}^2 w}{\mathrm{d}x^2}, \tag{9}$$

so that, for a given x, the maximum stress is at the surface of the ice, $z = \pm h/2$. From equation (8), it is a simple matter to show that the maximum stress in the two floes occurs at $X = \pm\pi/2\sqrt{2}$ and that this stress has magnitude

$$|\sigma_{\max}| = \frac{E}{2(1-\nu^2)} \frac{h^2}{\ell^2} \frac{e^{-\pi/4}}{2\sqrt{2}}. \tag{10}$$

[15] For rafting to be possible we require that this stress be less than the maximum stress that can be supported by the material, or the tensile strength, σ_m. In order to insure that this condition is satisfied the nondimensional thickness must obey

$$H < H_c \equiv 2^{5/4} e^{\pi/8} \left[1-\nu^2\right]^{1/2} \left(\frac{\sigma_m}{E}\right)^{1/2}. \tag{11}$$

We note that dimensional analysis leads us to expect that $H_c = f(\sigma_m/E,\nu)$. However, the functional form of f cannot be determined without this detailed calculation.

[16] In dimensional terms, equation (11) reads

$$h < h_c = \frac{8}{3} e^{\pi/2} \frac{1-\nu^2}{\rho_l g} \frac{\sigma_m^2}{E}, \tag{12}$$

which has the same dependence on material properties as the result given by *Parmerter* [1975] and reproduced in equation (1). However, the prefactor in equation (12) is approximately 12.8 rather than the 14.2 reported by *Parmerter* [1975]. This is because Parmerter's calculation allowed the overridden ice to be partially submerged. The additional weight of the water on the submerged ice causes a reduced curvature when the floes are on the brink of rafting thereby allowing thicker ice to raft. The small discrepancy between the prefactors produced with these two models shows that our neglect of the partial submergence of one of the floes does not significantly affect the predicted critical thickness at which simple rafting ceases. We shall therefore continue to neglect this partial submergence in the other calculations presented here.

Table 1. Typical Values From the Literature for the Mechanical Properties of Ice[a]

Ice Type	Material Properties			Reference
	E (*GPa*)	ν	σ_m (*MPa*)	
Fresh	0.3–12	0.33	1–3	*Hobbs* [1974] and *Schulson* [1999]
Sea	0.1–0.9	—	0.1–0.4	*Weeks and Anderson* [1958]
Sea	1	0.29	0.4	*Evans and Untersteiner* [1971]

[a]Here, E is the Young's modulus, ν the Poisson ratio, and σ_m the yield strength of the ice.

2.2. Comparison to Field Observations

[17] We can use the typical values given in Table 1 for the material properties of ice to give an estimate for h_c. Because these properties are sensitive functions of temperature and salinity, we take care to use estimates of σ_m and E observed in the same sample: mixing values from a weak sample (small σ_m) with those of a stiff sample (large E) can obfuscate the interpretation. We find that for sea ice 12 cm $\leq h_c \leq$ 21 cm, bracketing the transition thickness of 15 cm on the basis of field observations [*Weeks and Kovacs*, 1970].

[18] Above the critical thickness given by equation (12) we expect that the ice floes will break before rafting can occur and a pressure ridge will be formed from the blocks of ice that result. In particular, the maximum bending moment occurs a dimensional distance $\pi\ell/2\sqrt{2}$ away from the contact region and so we expect that a crack will form here and will be parallel to the edge of the floe. Moreover, we expect also that the blocks within the resulting pressure ridge should have this typical size. Because of the obvious difficulty of measuring the dimensions of ice blocks in a pressure ridge, there is little field data against which to confront this theoretical prediction. However, *Weeks and Kovacs* [1970] report that in one particular pressure ridge they found ice of thickness 30 cm and thickness/length ratio in the range 0.1–0.2. This compares well with the calculated ratio, based on the typical material properties of ice, which should lie in the range 0.07–0.13.

[19] On occasion, ice has been reported to raft even though it was well above the critical thickness given in equation (12); rafting was reported in ice up to 2 m thick by *Weeks and Kovacs* [1970] while *Melling et al.* [1993] inferred from their field survey the multiple rafting of four thin ice sheets accumulating a composite sheet approximately 6 m thick. *Babko et al.* [2002] suggested that this rafting in anomalously thick ice can be explained by two common complications: the presence of rubble on the ice helping to lift the floes over one another and/or multiple rafting events leading to thick ice made up of several thinner layers. Here we consider how these two possibilities modify the critical ice thickness for rafting given in equation (12).

2.3. Role of Rubble

[20] Consider two floes on the brink of rafting. If these floes are too thick to raft in the configuration shown in Figure 3, pieces will break off of them. The rubble created by this failed rafting will then lie on top of the subducting floe, weighing it down, and will also lie beneath the overriding floe, lifting it up, as shown schematically in Figure 4. Both *Hopkins et al.* [1999] and *Babko et al.* [2002] have suggested that this preloading will allow the rafting of thicker floes than might otherwise be possible. Here we quantify this suggestion to determine whether preloading can significantly alter the critical thickness at which rafting occurs.

[21] We imagine that the region $-L < X < L$ is covered in rubble of thickness αH. (In general, it is observed that ice floes are thinner near the edge at which rafting occurs, and hence we shall allow $\alpha \leq 1$ as a simple model of the nonuniformity in ice thickness.) The preloading of the ice due to the presence of rubble is accounted for by an additional force term in equation (2), corresponding to the buoyancy of the submerged rubble for $-L < X < 0$ or the weight of the overlying rubble for $0 < X < L$. Nondimensionalizing as before, the beam equation (6) now reads

$$\frac{\mathrm{d}^4 W}{\mathrm{d}X^4} + W = \begin{cases} 0 & |X| > L \\ (1-r)\alpha H, & -L < X < 0 \\ -r\alpha H, & 0 < X < L, \end{cases} \tag{13}$$

and is to be solved with the jump condition, equation (7) and the continuity of the first three derivatives of W at $X = 0, \pm L$. We find that the floe displacement is given by

$$W(X) = \frac{H}{2} \times \begin{cases} (1-\alpha)e^{\zeta}\cos\zeta + \alpha r e^{\eta}\cos\eta + (1-r)\alpha e^{\xi}\cos\xi, & X < -L \\ 2(1-r)\alpha + (1-\alpha)e^{\zeta}\cos\zeta + \alpha r e^{\eta}\cos\eta - (1-r)\alpha e^{-\xi}\cos\xi, & -L < X < 0 \\ -2r\alpha - (1-\alpha)e^{-\zeta}\cos\zeta + \alpha r e^{\eta}\cos\eta - (1-r)\alpha e^{-\xi}\cos\xi, & 0 < X < L \\ -(1-\alpha)e^{-\zeta}\cos\zeta - r\alpha e^{-\eta}\cos\eta - (1-r)\alpha e^{-\xi}\cos\xi, & X > L, \end{cases} \tag{14}$$

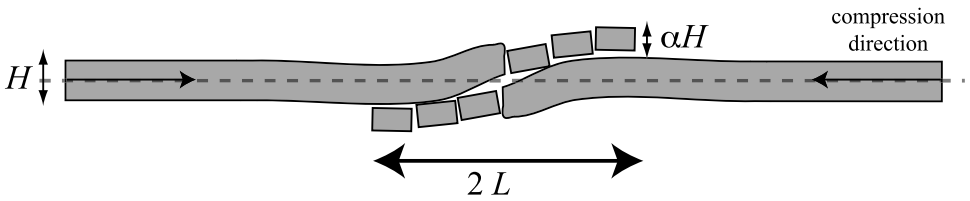

Figure 4. Schematic of two ice floes preloaded by rubble formed during failed rafting.

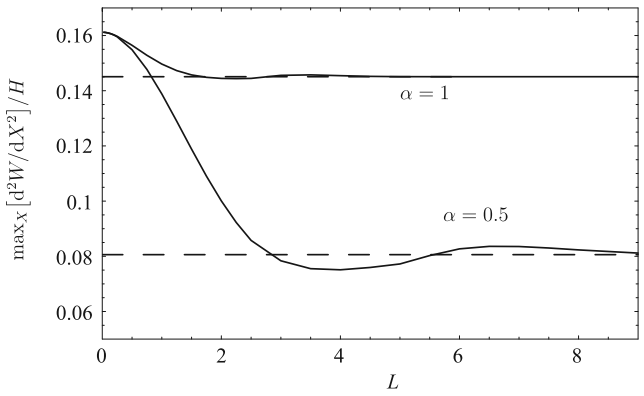

Figure 5. The maximum dimensionless curvature in ice floes loaded/supported with rubble of thickness αH over a horizontal extent of L. Here $r = \rho_s/\rho_l = 0.9$, as is typical of ice, and the values of α are indicated. The dashed lines show the asymptotic result, equation (16), which is valid for $L \gg 1$.

where $r \equiv \rho_s/\rho_l$ is the nondimensional density of the ice and

$$\xi \equiv \frac{X+L}{\sqrt{2}}, \quad \eta \equiv \frac{X-L}{\sqrt{2}}, \quad \zeta \equiv \frac{X}{\sqrt{2}}. \tag{15}$$

[22] Just as for rafting without rubble, the maximum stress in the floes is related to the maximum curvature in the floe via equation (9). This maximum curvature may be determined numerically using the solution in equation (14) for given values of r and L. The results in Figure 5, for $r = 0.9$ and two different values of the rubble thickness ratio α, show the maximum curvature as a function of the extent of rubble L. These curves demonstrate that as $L \to \infty$ the maximum curvature tends to a constant value. Considering the asymptotic limit $L \gg 1$, we find that the maximum value of the curvature, d^2W/dX^2, occurs at either $X \approx L - \pi/2^{3/2}$ (when $1-\alpha < r\alpha$) or $X \approx \pi/2^{3/2}$ (when $1-\alpha > r\alpha$). Therefore, the maximum curvature throughout the system for large L is

$$\max_X \left[\frac{d^2W}{dX^2}\right] \approx \frac{Hf(r,\alpha)}{2\sqrt{2}} e^{-\pi/4}, \tag{16}$$

where

$$f(r,\alpha) \equiv \begin{cases} 1-\alpha, & \alpha < (1+r)^{-1} \\ r\alpha, & \alpha > (1+r)^{-1}, \end{cases} \tag{17}$$

and

$$\max_x [g(x)]$$

denotes the maximum absolute value of the function $g(x)$ over all values of the variable x (which is also commonly denoted by $||g(x)||_\infty$).

[23] Following the same procedure that led to equation (11), we find that the maximum nondimensional thickness, H_c^*, for which rafting can occur is

$$H_c^* = \frac{2^{5/4} e^{\pi/8} (1-\nu^2)^{1/2}}{f(r,\alpha)^{1/2}} \left(\frac{\sigma_m}{E}\right)^{1/2}, \tag{18}$$

which is precisely the same result as presented in equation (11) modified by a factor $f(r, \alpha)^{-1/2}$, i.e., $H_c^* = f(r,\alpha)^{-1/2} H_c$. We note also that in the absence of rubble $\alpha = 0$ and $f(r,0) = 1$ so that equation (18) reduces to equation (11) as expected. In dimensional terms we have

$$h_c^* = f(r,\alpha)^{-2} h_c, \tag{19}$$

where h_c is as in equation (12). For $\alpha \leq 1$ and $r < 1$, $f(r, \alpha) < 1$ so that $h_c^* > h_c$: the presence of rubble does indeed increase the maximum thickness for which ice floes can raft.

[24] For ice, $r \approx 0.9$ and rubble with the same thickness as the ice itself ($\alpha = 1$) will lead to an increase of about 25% in the maximum thickness for which rafting can occur ($h_c^* \approx 1.23 h_c$). By varying α, however, we can obtain a significantly larger h_c: for a given value of r the minimum value of f is $r(1+r)^{-1}$ and is attained with $\alpha = (1+r)^{-1}$. For ice this minimum value is $f(0.9,0.526) \approx 0.474$ so that $h_c^* \approx 4.46 h_c$ and hence we might expect to see rafting in ice of thickness up to $h \approx 95$ cm.

2.4. Multiple Rafting Events

[25] *Melling et al.* [1993] and *Babko et al.* [2002] suggested that apparent rafting in thick ice may, in fact, be the result of multiple rafting events. We expect that two sandwich ice floes formed by the rafting of several thinner floes may themselves raft when their total thickness is greater than the critical thickness given in equation (12) because such sandwiches are more flexible than a single floe with the same thickness. In this section we quantify this expectation using scaling arguments.

[26] A sandwich consisting of n floes (each of thickness h/n) has an effective bending stiffness

$$B' = n \frac{E(h/n)^3}{12(1-\nu^2)} = n^{-2} B, \tag{20}$$

under the assumption that its constituent floes are free to slip past one another. (We note that this estimate is a lower bound for the effective bending stiffness of a composite sheet. We use this lower bound because the hypothesis is that the increased flexibility increases the critical thickness h_c.) The effective natural length scale for deformations of such a composite floe is then

$$\ell' = (B'/\rho_l g)^{1/4} = n^{-1/2} \ell. \tag{21}$$

[27] For two of these sandwiches to ride over one another requires a displacement of each floe of $w \sim h$ (where $\sim$ means "scales as") so that the curvature of each floe $\sim h/\ell'^2 = nh/\ell^2$. However, because the floes may slip past one another, the stress profile of equation (9) only holds over the thickness of the individual floes, h/n, and the maximum stress within each becomes

$$\sigma \sim Eh/n \times nh/\ell^2 = Eh^2/\ell^2, \tag{22}$$

independent of n. Rafting requires that $\sigma < \sigma_m$ and so (on accounting for the various constants) we recover equation

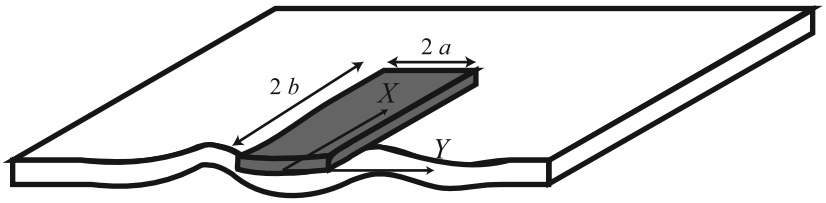

Figure 6. Schematic illustration of a $2a \times 2b$ rectangular finger overlying a floe.

(12): contrary to expectation there is no dependence of the maximum rafting thickness on n. This surprising result is due to the fortuitous cancellation of n in equation (22).

[28] Combining this result with equation (19) from section 2.3 we conclude that rafting in ice thicker than around 1 m cannot be explained solely by the presence of rubble on the ice or multiple rafting events and must, at least in part, be attributed to variations in the mechanical properties of sea ice, and its complex rheology and geometry [*Rothrock and Thorndike*, 1984]. This seems plausible given that

$$h_c \sim \sigma_m^2/E$$

so that small variations in σ_m in particular may be amplified. In this regard, we note that the data presented by *Weeks and Anderson* [1958] shows that σ_m is a very sensitive function of salinity while E is more sensitive to temperature. It therefore seems possible that σ_m and E may vary in a manner that leads to values of h_c that are considerably larger than reported here.

3. Finger Rafting

[29] It is observed that in addition to simple rafting, there is another form of rafting in which ice floes alternately ride over and under one another forming a series of interlocking fingers. Hence, this form of rafting is known as finger rafting [e.g., *Green*, 1970]. An example of finger rafted ice is shown in Figure 2.

[30] Just as there was a critical thickness above which simple rafting is not possible, we expect that there might also be a critical ice thickness above which simple rafting, rather than finger rafting, will take place. On the basis of intuition gleaned from many field observations, *Weeks and Kovacs* [1970] suggest that for ice thicker than around 10 cm, finger rafting becomes rare, presumably resulting instead in simple rafting. Here, we are concerned with explaining this behavior rather than the mechanism for finger rafting itself, which is discussed elsewhere [*Vella and Wettlaufer*, 2007].

[31] As we found with the rafting/ridging transition discussed earlier, we expect that the equilibrium configuration of the ice required for finger rafting to occur may cause the stresses within the ice to exceed the maximum value that it can support, σ_m. The stresses within the ice are given by the two-dimensional versions of equation (9) [*Mansfield*, 1989], which may be written as

$$\sigma_X = -\frac{Ez}{1-\nu^2}\left(\frac{\partial^2 w}{\partial x^2} + \nu\frac{\partial^2 w}{\partial y^2}\right).$$

[32] The expressions for these stresses are related to the expressions for the (dimensional) bending moments in the X and Y directions at a point (X, Y), which are given by [*Mansfield*, 1989]

$$\begin{aligned} m_{XX}(X,Y) &= -\frac{B}{\ell}\left(\frac{\partial^2 W}{\partial X^2} + \nu\frac{\partial^2 W}{\partial Y^2}\right) \\ m_{YY}(X,Y) &= -\frac{B}{\ell}\left(\nu\frac{\partial^2 W}{\partial X^2} + \frac{\partial^2 W}{\partial Y^2}\right). \end{aligned} \tag{23}$$

[33] (The subscripts here denote the directions of the bending moment.) The maximum stress through the ice thickness may then be written

$$|\sigma_{\max}| = \frac{6}{h^2}\max(m_{XX}, m_{YY}). \tag{24}$$

Searching for maximal stresses therefore corresponds to searching for maximal bending moments.

[34] The advantage of this approach is that explicit formulae for the moments generated by a point force acting on a semi-infinite plate on an elastic foundation (equivalent to a floating plate) are given by *Kerr and Kwak* [1993]. (Their expression for the displacement $W(X, Y; X_0, Y_0)$ at (X, Y) caused by a point force acting at (X_0, Y_0) is given in Appendix A. The corresponding formulae for the moments are more convoluted and are therefore omitted here.)

[35] For simplicity, we will consider the moments generated in a floating plate when a rectangular finger of width $2a$ and length $2b$ from another floe sits on top of it. Thus, as depicted in Figure 6, the finger is imagined to occupy the region $0 \le X \le 2b$, $|Y| \le a$. Each infinitesimal element of the protruding finger contributes to the bending moment of the overridden floe. Since the equation governing the displacement of the ice is linear, we can sum these moments to give the moment due to the presence of the finger. An element of width δX_0 and length δY_0 contributes a force $f = -\rho_s g h \ell^2 \delta X_0 \delta Y_0$. Integrating over the rectangle $0 \le X_0 \le 2b$, $|Y_0| \le a$ gives us the total bending moments experienced by the overridden floe, which we may write as

$$\begin{aligned} m_{XX}(X,Y) &\equiv \frac{\rho_s}{\rho_l}\frac{Bh}{\ell^2}\mu_x(a,b,X,Y) \\ m_{YY}(X,Y) &\equiv \frac{\rho_s}{\rho_l}\frac{Bh}{\ell^2}\mu_y(a,b,X,Y). \end{aligned}$$

[36] The functions μ_x and μ_y represent the dimensionless bending moments in the overridden floe caused by the protruding finger. These functions may be evaluated by numerical quadrature. Our numerical results are in perfect agreement with those tabulated by *Nevel* [1965], over his limited range of values of a and b. We find numerically that

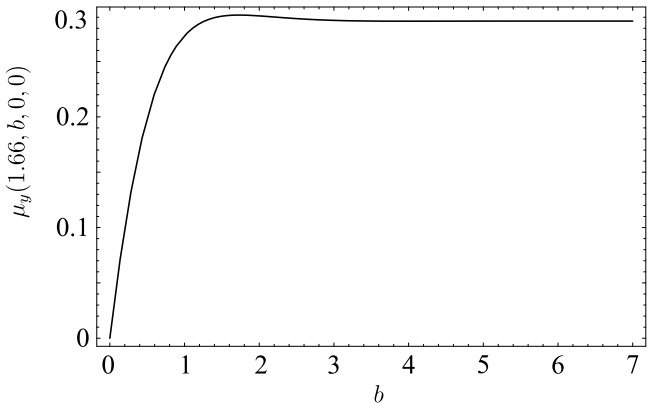

Figure 7. Plot of $\mu_y(1.66, b, 0, 0)$ as a function of the finger semilength b. Here, $\nu = 0.33$.

the largest moments generated are in $\mu_y(a, b, 0, 0)$. From this result, we expect that the failure of the ice floe should be manifested in a crack perpendicular to the floe edge. This is contrary to the failure of simple rafting in which a crack formed parallel to the free edge of the ice floe.

[37] To find a critical thickness above which finger rafting can no longer occur, we seek μ_∞; the maximum value of $\mu_y(a, b, 0, 0)$. *Vella and Wettlaufer* [2007] argued that the wavelength, λ, of the fingering pattern is linearly proportional to the characteristic length ℓ and found that

$$\lambda \approx 6.64\ell. \tag{25}$$

(A brief justification of this result is given in Appendix A.) Since we expect individual fingers to have a dimensional width of $\lambda/2$ we choose $a = \lambda/4\ell \approx 1.66$ and calculate $\mu_y(a, b, 0, 0)$ as the finger length, $2b\ell$, varies.

[38] Figure 7 shows the numerically computed values of $\mu_y(1.66, b, 0, 0)$ thereby demonstrating that there is indeed a maximum value, $\mu_\infty \approx 0.29$ for $\nu = 0.33$. Given this maximum moment we require that

$$\sigma_m > \frac{6}{h^2}\frac{\rho_s}{\rho_l}\frac{Bh}{\ell^2}\mu_\infty, \tag{26}$$

for the finger to be able to grow indefinitely without the ice beneath it breaking. This condition is satisfied provided that

$$H < \left[\frac{\rho_l}{\rho_s}\frac{2(1-\nu^2)}{\mu_\infty}\right]^{1/2}\left(\frac{\sigma_m}{E}\right)^{1/2} \approx 2.6\left(\frac{\sigma_m}{E}\right)^{1/2}. \tag{27}$$

[39] The critical thickness at which finger rafting becomes impossible scales with σ_m/E in precisely the same way as the critical thickness at which simple rafting gives way to ridging. However, the prefactor is different (and smaller!) suggesting that for a given value of σ_m/E we may be able to transition between finger rafting, simple rafting and ridging simply by varying the ice thickness. The condition in equation (27) may be recast in dimensional terms as

$$h < \frac{\rho_l}{\rho_s}\frac{1-\nu^2}{3\rho_s g\mu_\infty^2}\frac{\sigma_m^2}{E}. \tag{28}$$

Taking typical values for the material properties of sea ice, we find that this transition thickness lies in the interval

$$4\,\text{cm} \leq h_c \leq 8\,\text{cm}. \tag{29}$$

[40] Given the spatiotemporal evolution of the structure of thin ice [*Wettlaufer et al.* 1997], this estimate is in very good agreement with the observation of W. F. Weeks (On Sea Ice, submitted to University of Alaska Fairbanks Press, 2008) that finger rafting becomes rare for ice thicknesses above 10 cm. Our theoretical prediction is also consistent with most of the field observations collated by *Vella and Wettlaufer* [2007], for which finger rafting is observed in ice of thickness up to around 6 cm. This also provides some quantitative support for the statement of *Weeks and Kovacs* [1970, p. 22] that "Although less striking when observed from the air, simple rafting of thin ice... is actually more common than finger rafting."

[41] We are aware of only one reported instance when finger rafting was inferred to be responsible for features in much thicker ice than our theory predicts is possible using physical parameters typical for sea ice: the summertime observations of *Mahoney et al.* [2004]. We believe that such a discrepancy may be accounted for by similar arguments to those given in our earlier discussion of simple rafting.

[42] Because the maximum bending moment in the floe is $\mu_y(a, b, 0, 0)$, we expect that a crack will form in the overridden ice perpendicular to its edge. Once the overridden ice is broken, our model no longer applies: what happens next to the overlying finger is therefore beyond the scope of this work. However, since finger rafting can no longer occur, the system must find another way to accommodate deformation. Perhaps the presence of a crack means that the finger breaks through the floe and is subducted beneath along with the remainder of the floe in simple rafting? We expect that above the critical thickness a finger might start to grow but will fall through the underlying ice once it has reached a length of at most 4ℓ, which is on the same order as the finger width. We are unaware of observations wherein finger rafting metamorphoses into simple rafting against which to check this picture.

4. Conclusions

[43] In this paper we have studied the collisions of ice floes from the context of thin plate theory. We focused on the three main types of deformation that result from the collision of two floes. By considering the forces induced by these different deformations we provided quantitative bounds on the different ice thicknesses for which each of these deformation patterns is observed. In particular, by plotting the dimensionless conditions in equations (11) and (27) on the same graph, we obtain a regime diagram showing the values of σ_m/E and H for which finger rafting, simple rafting and pressure ridging should be observed. Such a regime diagram is shown in Figure 8.

[44] We end by noting that although finger rafting has been observed in floating sheets of wax [*Vella and Wettlaufer*, 2007] we do not expect this regime diagram to necessarily be quantitatively accurate for all other materials.

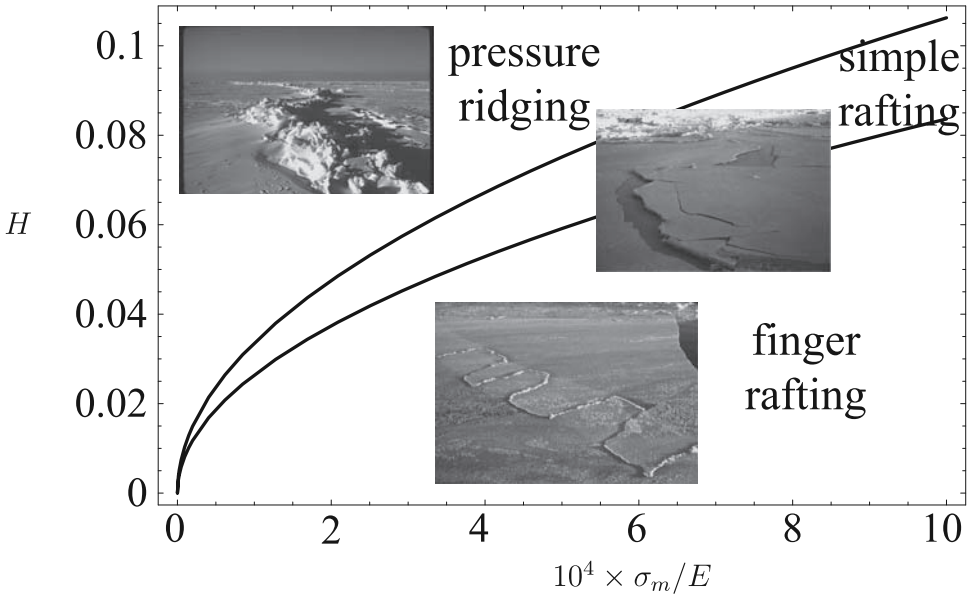

Figure 8. Regime diagram showing the values of σ_m/E and H for which we expect to observe each of the deformation types observed. Photographs courtesy of Weeks (submitted manuscript, 2008).

Ice is unusual because it typically has $\sigma_m/E < 10^{-3}$: the transitions between different regimes therefore occur with $H \ll 1$, and thus thin plate theory is valid. To the extent that this is the case for other materials our analysis will have predictive relevance for them as well. It is hoped that the swath of other geophysical and engineering settings in which this framework is valid will be fruitfully explored using the ideas underlying these basic patterns of deformation and failure.

Appendix A: Floe Displacement Due to a Point Force

[45] Here we give the Green's function for the displacement of a semi-infinite plate on an elastic foundation or, equivalently, for the displacement of a semi-infinite floe. This result was derived by *Kerr and Kwak* [1993]. The displacement, $W(X, Y; X_0, Y_0)$, due to the application of a nondimensional point force $F \equiv f/\rho_l g\ell^3$ at the point (X_0, Y_0) satisfies

$$\frac{\pi}{F}W(X,Y;X_0,Y_0) = -\frac{1}{2}\left[\mathrm{Kei}\left(R_0^-\right)+\mathrm{Kei}\left(R_0^+\right)\right] + \int_0^\infty A(X_0,\alpha)e^{-k_+X} \cdot\left\{\cos k_-X - \frac{k_+\left[2k_-^2+(1-\nu)\alpha^2\right]}{k_-\left[2k_+^2-(1-\nu)\alpha^2\right]}\sin k_-X\right\} \cdot\cos\alpha(Y-Y_0)\mathrm{d}\alpha \tag{A1}$$

[46] Here $\mathrm{Kei}(x)$ is the Kelvin function of zeroth order [*Abramowitz and Stegun*, 1964, p. 379], $R_0^\pm$ is given by

$$R_0^\pm = \left[(X\pm X_0)^2+(Y-Y_0)^2\right]^{1/2}, \tag{A2}$$

$k_\pm$ is given by

$$k_\pm = \left(\frac{1}{2}\left[\sqrt{\alpha^4+1}\pm\alpha^2\right]\right)^{1/2}, \tag{A3}$$

and

$$A(X_0,\alpha) = \frac{e^{-k_+X_0}}{\sqrt{\alpha^4+1}}\frac{2k_+^2-(1-\nu)\alpha^2}{4k_+^2\left[k_-^2+(1-\nu)\alpha^2\right]-(1-\nu)^2\alpha^4} \cdot\left[k_-\left(k_-^2+k_+^2+\nu\alpha^2\right)\cos k_-X_0 - k_+\left(k_-^2+k_+^2-\nu\alpha^2\right)\sin k_-X_0\right]. \tag{A4}$$

(We note that there is a typographical error in the expression for $k_\pm$ given by *Vella and Wettlaufer* [2007]. The correct expression appears above.) This expression for W can be differentiated to give the bending moment within the floe from equation (23).

[47] Here we also briefly discuss the prediction for the wavelength of finger rafting given by equation (25). *Vella and Wettlaufer* [2007] argued that finger rafting occurs when a small portion of one floe protrudes on top of the other. This then causes a point loading of both floes: one is lifted up and the other pushed down. The amplitude of the disturbance will depend on the force applied (and hence the size of the overlying portion) making it difficult to compare this displacement to, say, the floe thickness. However, we can plot the normalized vertical displacement of the floes, as shown in Figure A1. This shows that the vertical deflection of each floe decays and also oscillates away from the origin. Furthermore, because the two floes are subject to forces of opposite signs, these oscillations are exactly out of phase. Upon further compression, therefore, we may expect that the two floes tear one another leaving a finger width that is determined by

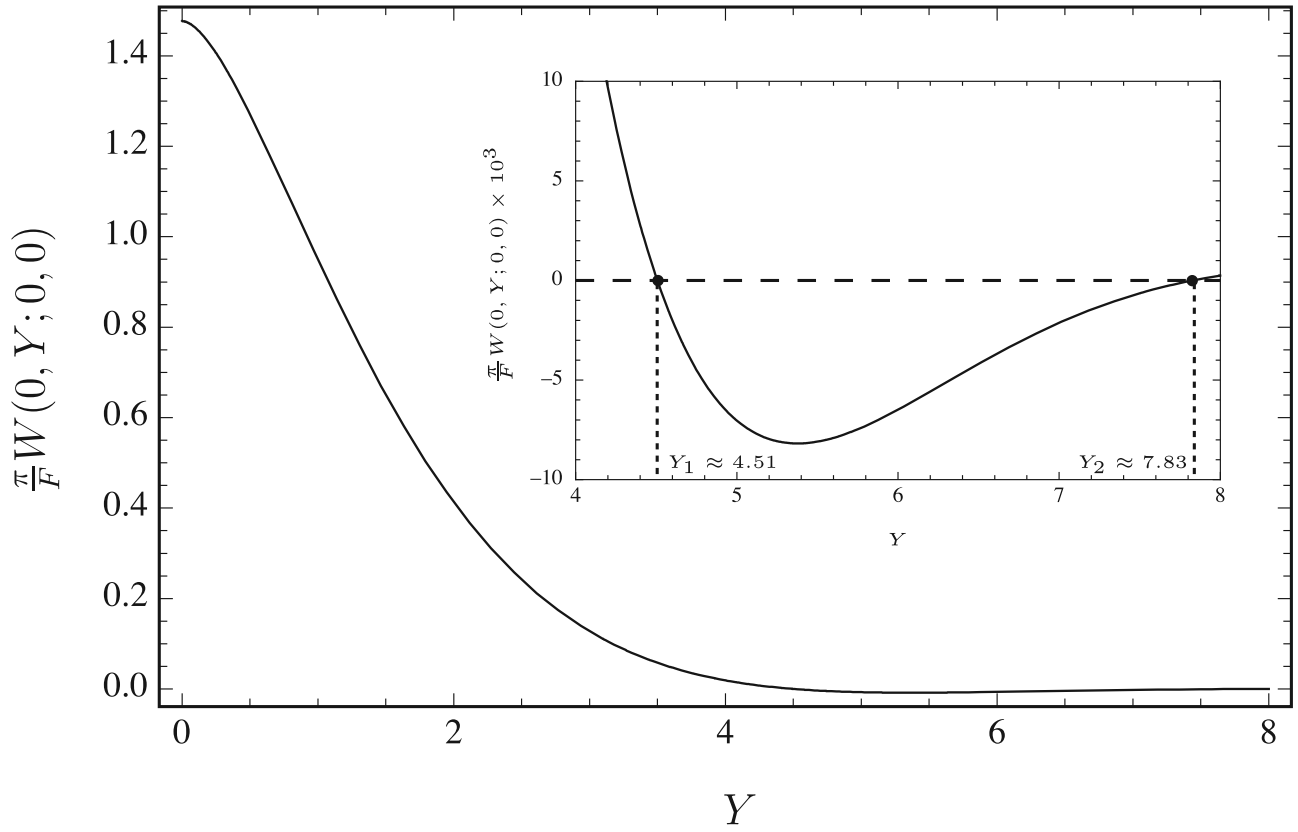

Figure A1. The edge displacement, $W(0, Y; 0, 0)$, of a floe under the action of a point force F at the origin. The inset shows the first two zeros of W, Y_1, and Y_2, which determine the wavelength of finger rafting given in equation (25) via $\lambda = 2(Y_2 - Y_1)\,\ell$. Here $\nu = 1/3$.

the distance between the first two roots of $W(0, Y; 0, 0) = 0$, as illustrated in Figure A1. Doubling this finger width gives the finger rafting wavelength provided by equation (25). *Vella and Wettlaufer* [2007] also suggest that though the displacement between these two zeros is small, it is enough to "prime" the two floes to run over and under one another at these points, thus allowing the finger rafting to the propagate as a "zipper" along the entire edge of the floes.

[48] **Acknowledgments.** The authors would like to acknowledge conversations, feedback, technical support and facilities and photographs, variously from N.J. Balmforth, D. Bercovici, K. Bradley, H. Eicken, W.F. Weeks, J.A. Whitehead and L.A. Wilen. We thank J.F. Nye for encouraging us to clarify the arguments surrounding and leading to Figure A1. Support for this research, which began at the summer program in Geophysical Fluid Dynamics at Woods Hole Oceanographic Institution, was provided by NSF OCE0325296. JSW is also supported by NSF OPP0440841 and DOE DE-FG02-05ER15741. DV is grateful to Trinity College, Cambridge, for its support.

References

Abramowitz, M., and I. A. Stegun (1964), Handbook of Mathematical Functions with Formulas, Graphs, and Mathematical Tables, 1046 pp., Dover, New York.

Babko, O., D. A. Rothrock, and G. A. Maykut (2002), Role of rafting in the mechanical redistribution of sea ice, *J. Geophys. Res.*, *107*(C8), 3113, doi:10.1029/1999JC000190.

Evans, R. J., and N. Untersteiner (1971), Thermal cracks in floating ice sheets, *J. Geophys. Res.*, *76*, 694–703.

Green, J. C. (1970), Finger-rafting in fresh-water ice: Observations in Lake Superior, *J. Glaciol.*, *9*, 401–404.

Hobbs, P. V. (1974), Ice Physics, 837 pp., Oxford Univ. Press.

Hopkins, M. A. (1998), Four stages of pressure ridging, *J. Geophys. Res.*, *103*, 21,883–21,891.

Hopkins, M. A., J. Tuhkuri, and M. Lensu (1999), Rafting and ridging of thin ice sheets, *J. Geophys. Res.*, *104*, 13,605–13,613.

Kerr, A. D., and S. S. Kwak (1993), The semi-infinite plate on a Winkler base, free along the edge, and subjected to a vertical force, *Arch. Appl. Mech.*, *63*, 210–218.

Mahoney, A., H. Eicken, L. Shapiro, and T. C. Grenfell (2004), Ice motion and driving forces during a spring ice shove on the Alaskan Chukchi coast, *J. Glaciol.*, *50*, 195–207.

Mansfield, E. H. (1989), The Bending and Stretching of Plates, 227 pp. Cambridge Univ. Press.

Matsuoka, K. (1972), The mechanics of fracture of sea ice in leads, M. S. thesis, 56 pp., Univ. of Washington, Seattle.

Melling, H., D. R. Topham, and D. Riedel (1993), Topography of the upper and lower surfaces of 10 hectacres of deformed sea ice, *Cold Reg. Sci. Technol.*, *21*, 349–369.

Nevel, D. E. (1965), A semi-infinite plate on an elastic foundation, Tech. Rep. 136, Cold Regions Res. and Eng. Lab., Hanover, N. H.

Parmerter, R. R. (1975), A model of simple rafting in sea ice, *J. Geophys. Res.*, *80*, 1948–1952.

Parmerter, R. R., and M. D. Coon (1972), A model of pressure ridge formation in sea ice, *J. Geophys. Res.*, *77*, 6565–6575.

Rothrock, D. A. (1975), The mechanical behaviour of pack ice, *Annu. Rev. Earth Planet. Sci.*, *3*, 317–342.

Rothrock, D. A., and A. S. Thorndike (1984), Measuring the sea ice-floe size distribution, *J. Geophys. Res.*, *89*, 6477–6486.

Schulson, E. M. (1999), The structure and mechanical behaviour of ice, *J. Miner. Metals Mater. Soc.*, *51*, 21–27.

Thorndike, A. S., D. A. Rothrock, F. A. Maykut, and R. Colony (1975), The thickness distribution of sea ice, *J. Geophys. Res.*, *80*, 4501–4513.

Vella, D., and J. S. Wettlaufer (2007), Finger rafting: A generic instability of floating elastic sheets, *Phys. Rev. Lett.*, *98*, 088303.

Weeks, W. F., and D. L. Anderson (1958), An experimental study of strength of young sea ice, *EOS Trans. AGU*, *39*, 641–647.
Weeks, W. F., and A. Kovacs (1970), On pressure ridges, *CREEL Rep. IR505*, Cold Reg. Res. and Eng. Lab., 59 pp., Hanover, N. H.
Wensnahan, M., D. A. Rothrock, and P. Hezel (2007), New arctic sea ice data from submarines, *EOS Trans. AGU*, *88*, 55–56.
Wettlaufer, J. S., M. G. Worster, and H. E. Huppert (1997), The phase evolution of young sea ice, *Geophys. Res. Lett.*, *24*, 1251–1254.

D. Vella, Institute of Theoretical Geophysics, Department of Applied Mathematics and Theoretical Physics, University of Cambridge, Wilberforce Road, Cambridge CB3 0WA, UK. (d.vella@damtp.cam.ac.uk)
J. S. Wettlaufer, Department of Geology and Geophysics and Department of Physics, Yale University, New Haven, CT 06520-8109, USA. (john.wettlaufer@yale.edu)